BUTTERWORTH HEINEMANN

Polymer Vol. 36 No. 6, pp. 1157–1165, 1995

0032-3861/95/$10.00+0.00

Two-dimensional small-angle X-ray scattering studies on oriented poly(ethylene terephthalate) films

Ulrich Göschel*
Max-Planck-Institut für Polymerforschung, Postfach 3148, 55021 Mainz, Germany
(Received 24 January 1994)

The supermolecular structure of uniaxially drawn ($5.4 \leqslant \lambda \leqslant 7.3$) poly(ethylene terephthalate) (PET) films exhibiting a very high orientation of the chain molecules was investigated by two-dimensional small-angle X-ray scattering studies. Depending on the drawing history, the intensity distribution along the meridional layer line as well as at the equator was analysed. With the incident beam perpendicular to the film plane, the drawn PET samples revealed so-called two-point or four-point meridional scattering patterns. From the intensity distribution along the meridional layer line, a lamellar structure with stacks of comparatively short crystalline lamellae, both perpendicular and inclined with respect to the drawing direction, was concluded. Parameters like the inclination angle, the lamellar periodicity along the drawing direction as well as the normal to the lamellae and the half-widths of the meridional layer line reflexes were determined. As a result, large orientation changes in the normal to the lamellae with regard to the drawing direction during stretching were found. Even for already highly oriented and semicrystalline PET structures, further drawing changes the orientation of the lamellae dramatically.

(Keywords: poly(ethylene terephthalate); uniaxial drawing; high chain orientation)

INTRODUCTION

The microstructure of drawn semicrystalline polymers is given by an alternating spatial arrangement of disordered and ordered regions[1]. Crystallites are the ordered structural elements with the smallest size. Their periodic arrangement can form a lamella. Stacks of short lamellae are often regarded as fibrils. Two principal structural models (fibrillar and lamellar models) can be used to describe the superstructure and the deformation mechanism under loading[2]. By means of small-angle X-ray scattering (SAXS) studies, a dimension range from about 30 up to several hundred angstroms is detectable and corresponds to the structural features mentioned above.

SAXS patterns of uniaxially drawn semicrystalline polymers provide long-period interferences owing to a nearly periodic arrangement of disordered and ordered regions along the drawing direction[1]. The main information is given by the scattering intensities along the meridian and the meridional layer line. In the case of submicroscopic voids, caused by phases of lower density arranged between the fibrils, additional scattering intensities along the equator can be observed[3,4].

In previous studies the uniaxial drawing behaviour of poly(ethylene terephthalate) (PET)[5] and the structural transition from an isotropic and non-crystalline structure into a highly oriented and non-crystalline structure and from that into a highly oriented and semicrystalline structure with a degree of order ($L_{\bar{1}05}/L$) of about 30% were discussed[6]. $L_{\bar{1}05}$ and L denote the crystal thicknesses obtained from the half-width of the ($\bar{1}05$) reflection and the meridional SAXS long period, respectively. Despite the very high orientation of the chains, large differences in the thermomechanical and time-dependent deformation behaviour were found among samples with different pretreatments[7].

Several authors[2,8–11] have investigated the crystallization of oriented PET macromolecules. Fischer and Fakirov[8] reported an increase in the mosaic block sizes forming the crystalline layers and commented on their longitudinal mutual order. The volume fraction of the crystalline region was found to be only slightly affected by the annealing temperature. According to Biangardi and Zachmann[9], the PET structure obtained after crystallization depends mainly on the initial chain orientation before crystallization. Nobbs *et al.*[10] studied the change in molecular orientation and the shrinkage behaviour of oriented and partly crystalline PET during annealing in the temperature range 70–180°C. They found that shrinkage is associated with a misorientation of the amorphous regions, and further crystallization takes place independent of the misorientation process. Peszkin and Schultz[11] discussed the crystallization process in as-spun PET at an early stage during isothermal heat treatment. They described a fibrillar morphology with a fibril diameter ranging from 30 to 40 Å (1 Å = 0.1 nm) and found a two-stage crystallization process: the formation of defective fibrils followed by the formation of more-perfect crystals. Stockfleth *et al.*[2] examined rectangular PET strips. For uniaxially drawn PET they discussed the existence of lamellar stacks with different orientation angles with respect to the loading

* Present address: Tokyo University of Agriculture and Technology, Faculty of Technology, Department of Material Systems Engineering, Koganei, Tokyo 184, Japan

direction. It was reported that a lamellar separation occurred preferentially below or in the region of the glass transition temperature (T_g) at low strain. With increasing strain and temperature above T_g, slip deformation mechanisms became more important. At strains near the breaking point and temperatures below or in the region of T_g, Stockfleth *et al.*[2] observed the formation of microvoids.

To gain new insights into the structure formed under extreme uniaxial drawing conditions, we investigated highly oriented and semicrystalline PET structures by means of SAXS measurements. Previous studies on these structures revealed a draw ratio of $5.4 \leqslant \lambda \leqslant 7.3$, a degree of order of $26 \leqslant L_{\bar{1}05}/L \leqslant 39\%$, a Young's modulus of $13 \leqslant E \leqslant 17$ GPa, a stress at break of $800 \leqslant \sigma \leqslant 1000$ MPa, a birefringence of $0.202 \leqslant \Delta n \leqslant 0.249$ and a nearly perfect orientation of the c axis parallel to the drawing direction[5,6].

A two-dimensional detector in conjunction with point collimation was applied successfully to the SAXS investigation of oriented and semicrystalline PET structures. In comparison with a one-dimensional SAXS technique, the two-dimensional method provides additional information about the lamellar structures formed by inclined lamellae. Such structures often occur in semicrystalline polymers after drawing.

EXPERIMENTAL

Materials

By means of uniaxial drawing under various conditions[5], PET films with a high molecular chain orientation according to wide-angle X-ray scattering (WAXS), birefringence and mechanical measurements[5,6] were obtained. The multistep zone-drawing procedure used (*Figure 1*) started from nearly isotropic ($\Delta n = 0.5 \times 10^{-3}$) non-crystalline PET film strips with a thickness of 180 μm, a width of 2.8 mm and a molecular weight M_w of about 20 000 described by us elsewhere[5]. After the first drawing step below the glass transition in order to avoid crystallization (see samples 1 and 8), extremely large drawing stresses of up to 400 MPa were applied in the following steps (*Table 1*). During the second and third drawing steps a constant neck propagation velocity of 100 mm min^{-1} was used. Depending on the drawing temperatures and stresses applied, an average draw ratio of up to 7.3 was achieved. The sample designations in the present paper can also be found elsewhere[5-7].

Small-angle X-ray scattering (point collimation)

SAXS data were obtained using a Nicolet area detector combined with an 18 kW rotating Cu anode X-ray source (Rigaku RV-300). A graphite double monochromator was used. The collimator system provided a point focus with a beam diameter of about 1.0 mm. The resolution of the area detector was based on a matrix of 512×512 pixels with a pixel to pixel distance of 0.2 mm. The distance s between sample and detector was chosen to be 1250 mm. In order to obtain large scattering intensities, the recording time was lengthened and finally fixed at about 65 h for a laminated sample thickness of about 300 μm. Contrary to the 65 h recording time used, the visualization of the SAXS patterns themselves required only several hours. The data analysis was performed interactively by means of a VAXstation 3100 including a PV-wave software system. The scattering intensities were registered in transmission perpendicular to the (x_2, x_3) film plane, where x_1, x_2 and x_3 represent the sample coordinate

Table 1 Drawing conditions in the last drawing step of a multistep drawing process using a neck propagation velocity of 100 mm min^{-1}

Sample	Total number of drawing steps	Drawing temperature (°C)	Average maximum drawing stress σ_{max} (MPa)	Average maximum draw ratio λ
1	One	68	15[a]	4.3
2	Two	160	350[b]	6.3
3	Three	200	385[b]	7.1
4	Three	230	400[b]	7.3
5	Two	200	400[b]	7.2
8	One	23	[c]	4.2
9	Two	180	100	5.4

[a] Neck propagation velocity of 5.5 mm min^{-1}
[b] Stepwise increase in 50 MPa increments
[c] Drawing in a homogeneous temperature field with a neck propagation velocity of 0.71 mm min^{-1}

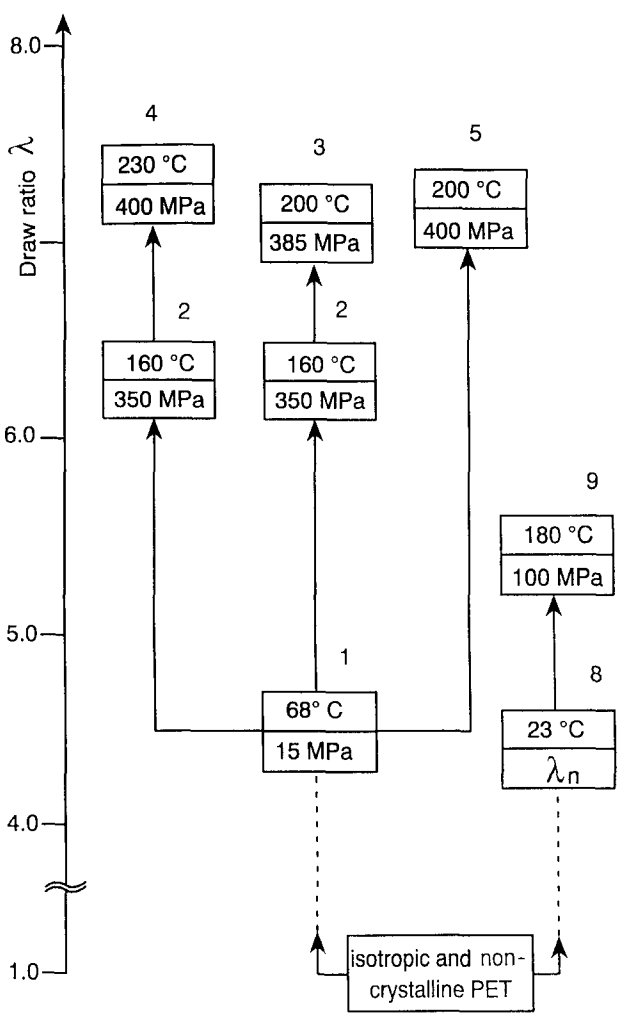

Figure 1 Multistep zone-drawing process to obtain the samples used in this study. The starting material was isotropic non-crystalline PET. Depending on the drawing conditions, an average draw ratio from 4.2 up to 7.3 was achieved. Each sample is characterized by the drawing temperature and the average maximum drawing stress applied at that temperature. In the case of samples 2, 3, 4 and 9, the drawing stress was increased step by step in 50 MPa increments

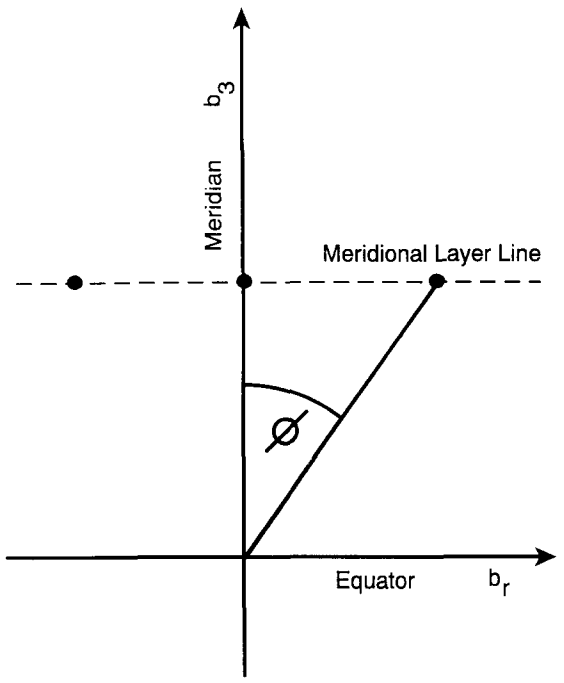

Figure 2 Coordinate system in reciprocal space

system with the axes parallel to the film thickness, width and drawing direction, respectively. The experiment provided the scattering intensities $I(b_2, b_3)$, where b_2 and b_3 denote the components of the scattering vector perpendicular and parallel to x_3, respectively, and where $|b| = (4\pi \sin\theta)/\lambda$ for a scattering angle of 2θ. The X-ray wavelength λ_{Cu} was 1.54 Å. In the case of cylindrical symmetry about the drawing direction x_3, corresponding to the b_3 axis in reciprocal space (*Figure 2*), the component of the scattering vector b_r is given by

$$b_r = \sqrt{b_1^2 + b_2^2} \tag{1}$$

Standard procedures were used for correction of the detector sensitivity, primary beam profile and background.

Small-angle X-ray scattering (slit collimation)

A Kratky compact camera (Anton-Paar KG, Graz), Ni-filtered CuKα radiation and a one-dimensional position-sensitive detector (OED-50-M from Braun GmbH, Garching) were used. The entrance slit was 60 μm wide and the sample to detector distance was about 240 mm. The measurements were performed with the incident beam parallel to the sample thickness (x_1) and the collimation slip perpendicular as well as parallel to the drawing direction (x_3). Because of sample anisotropy, only the smeared intensities were taken. The data were corrected for absorption and background scattering.

Using the collimation slit perpendicular to x_3 and with regard to equation (1), the Kratky camera measurement can provide the slit-smeared intensity function along the meridian[3]

$$\tilde{I}_{\perp}(b_3) \approx \int_0^B I(b_r, b_3)\, db_r \tag{2}$$

where B corresponds to the slit half-width in $Å^{-1}$.

To obtain the equatorial scattering intensities, the collimation slit has to be arranged parallel to the drawing direction (x_3). Then, according to Fischer *et al.*[1] and equation (1), the scattering experiment can yield

$$\tilde{I}_{\parallel}(b_r) \approx \int_0^B I(b_r, b_3)\, db_3 \tag{3}$$

RESULTS

SAXS (point collimation)

Poly(ethylene terephthalate) (PET) films were first drawn below the glass transition in order to obtain the oriented non-crystalline structures of samples 1 and 8 (*Figure 1* and *Table 1*)[5,6]. In this temperature range the drawing (denoted as cold drawing) is more sensitive to the conditions applied than at higher temperatures. Nevertheless, using the right choice of drawing parameters (stress, temperature and neck propagation velocity), a non-crystalline structure can be achieved. The lack of crystallites means weaker interactive forces between the chain molecules. In this case, further drawing can yield semicrystalline structures with an especially high chain orientation[5,6].

X-Ray studies showed that cold-drawn samples 1 and 8 are non-crystalline. Wide-angle X-ray scattering (WAXS) revealed no crystalline reflexes[6]. With respect to SAXS, a superstructure did not exist. Using the oriented and non-crystalline samples 1 and 8 as precursor materials for an additional drawing treatment at temperatures above the glass transition (T_g), the oriented and semi-crystalline structures of samples 2, 3, 4, 5 and 9 were obtained.

In *Figures 3–7* the SAXS contour plots, the three-dimensional intensity plots and the intensity distributions along the meridional layer line are represented for some of the PET structures mentioned above. The channels (r) in *Figures 3–7* correspond to the scattering angles (2θ) through

$$2\theta = \tan^{-1}\left(\frac{rz}{s}\right) \tag{4}$$

where z (= 0.2 mm) is the pixel to pixel distance of the detector and s (= 1250 mm) is the sample to detector distance.

In the contour plots of *Figures 3–7* the drawing direction is vertical. From the two-dimensional scattering patterns the intensities along the meridional layer line and the equator ($b_3 = 0$) can be seen. The centre of each pattern is the location of the primary beam. The three-dimensional intensity plots reveal the intensity distributions with respect to the (b_2, b_3) plane. At the bottom of each of *Figures 3–7* the intensity distribution along the meridional layer line is represented and provides the corresponding half-width of the peak intensity. Considering the distance between the meridional layer line and the equator, the lamellar periodicity L along the drawing direction, often denoted as the long period, is given by

$$L = \frac{2\pi}{q_{max,meridian}} \tag{5}$$

where $q_{max,meridian}$ is the scattering vector corresponding to the intensity maximum on the meridian. In the case of four-point scattering patterns, the inclination angle ϕ (see *Figure 2*) between the intensity maximum on the

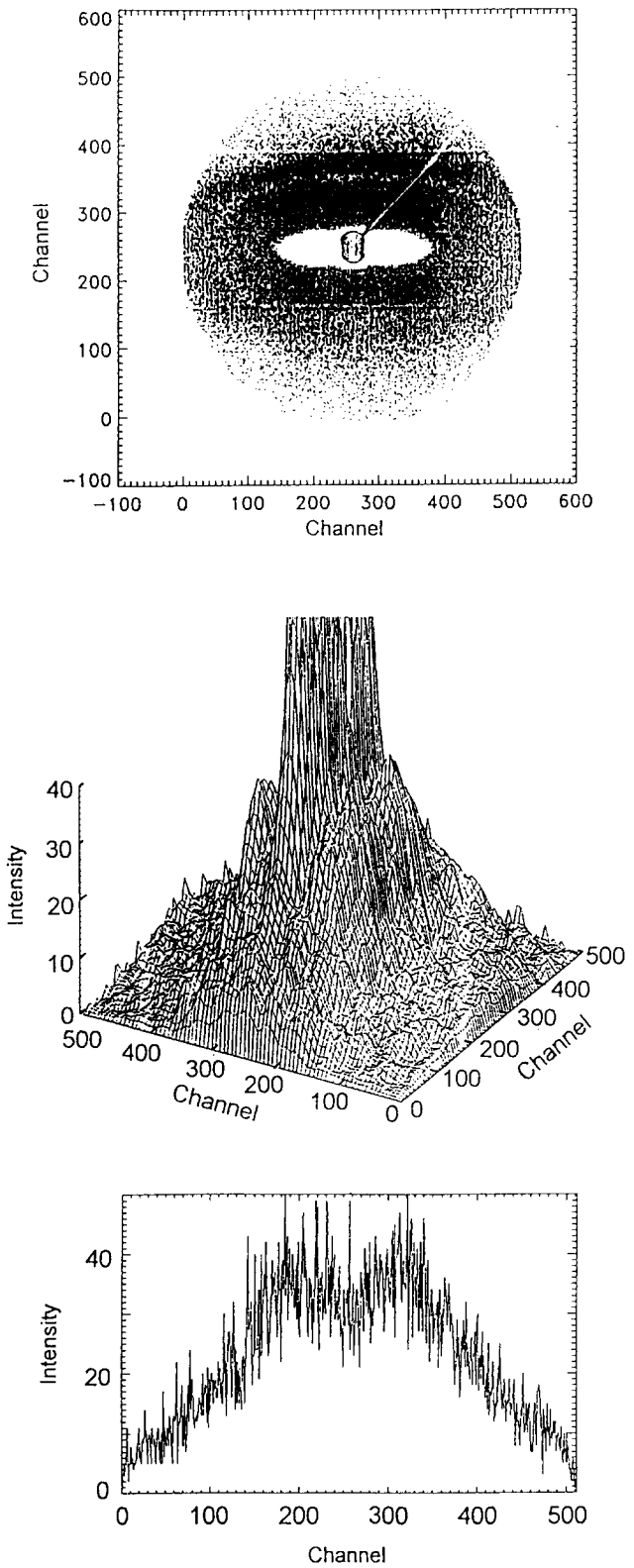

Figure 3 Two-dimensional SAXS pattern of an oriented semicrystalline PET sample with the incident beam perpendicular to the film plane. Represented are the contour plot, the three-dimensional intensity plot and the intensity distribution along the meridional layer line for sample 2

layer line and the meridian (b_3) can be ascertained. Then, for the lamellar periodicity L' with respect to the normal to the lamellae we have

$$L' = \frac{2\pi}{q'_{max}} \tag{6}$$

where

$$q'_{max} = \frac{q_{max,meridian}}{\cos\phi} \tag{7}$$

The SAXS parameters mentioned above are summarized in *Table 2*.

SAXS (slit collimation)

The intensity distribution along the meridian (b_3) and the equator (b_2) was studied by means of a Kratky camera.

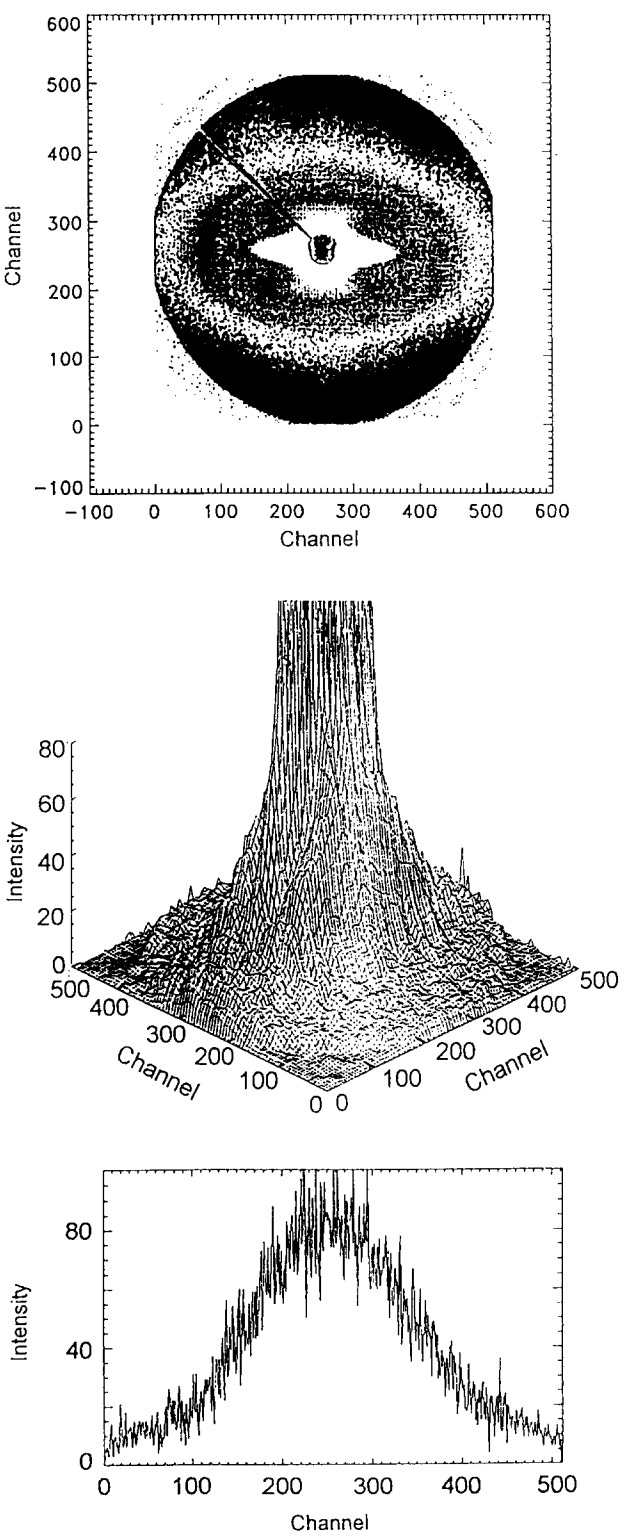

Figure 4 As for *Figure 3* but for sample 3

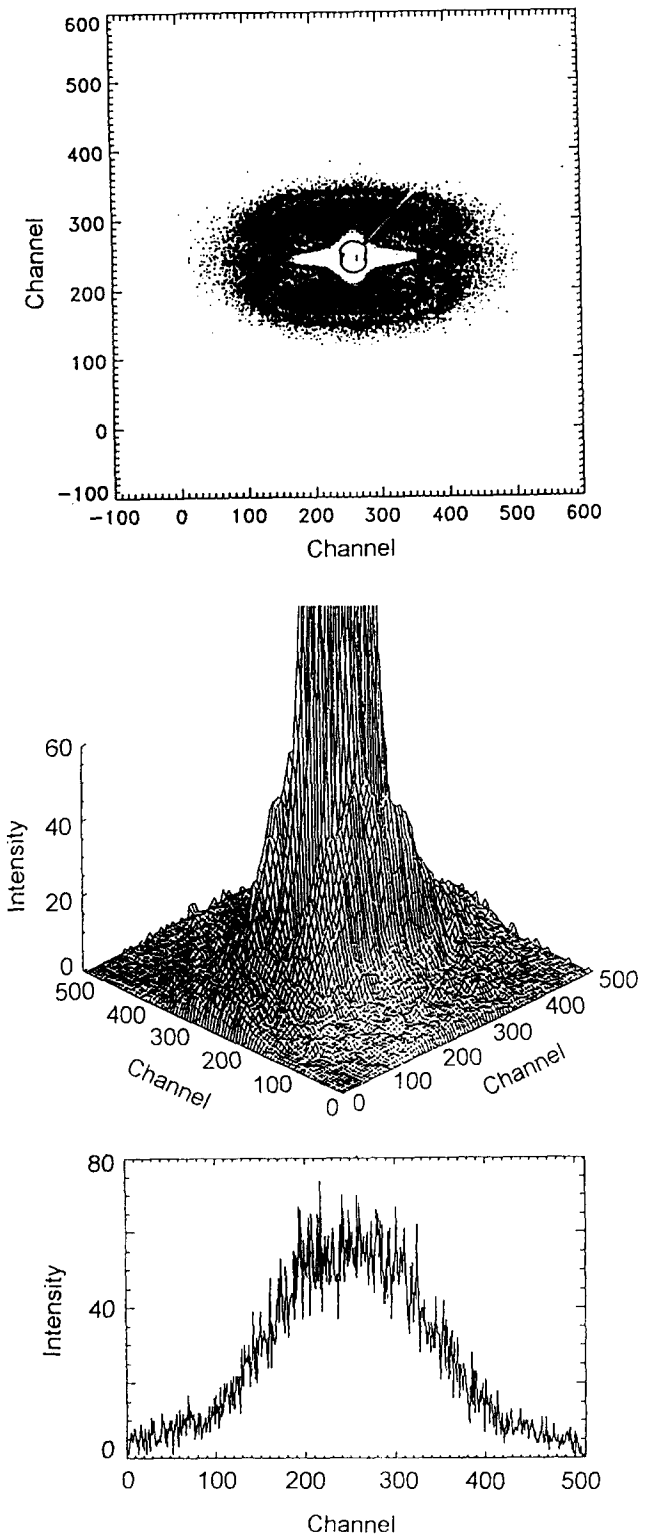

Figure 5 As for *Figure 3* but for sample 4

Table 2 Parameters determined from the two-dimensional SAXS patterns

Sample	Half-width of layer line intensity q (Å^{-1})	Inclination angle ( )	Long period L (nm)	Lamellar periodicity L' (nm)
2	0.185	45.4	15.0	10.6
3	0.124	0	16.6	16.6
4	0.129	0	16.0	16.0
5	0.202	52.0	15.4	9.3
9	0.202	47.8	14.2	9.5

Figure 8 shows the meridional scattering intensities of the semicrystalline PET samples (2, 3, 4, 5 and 9). From these scattering curves the long periods were determined using equation (5), the angular peak position and Bragg's law. The results are given in *Table 3*.

Kratky camera measurements with the collimation slit parallel to the drawing direction monitored the equatorial scattering intensities, as shown in *Figure 9*. These intensities are due to the occurrence of voids on the submicroscopic scale[3,4]. According to *Figure 9*, no peak maximum exists in the range $0.05 < q < 0.25\,\mathrm{nm}^{-1}$.

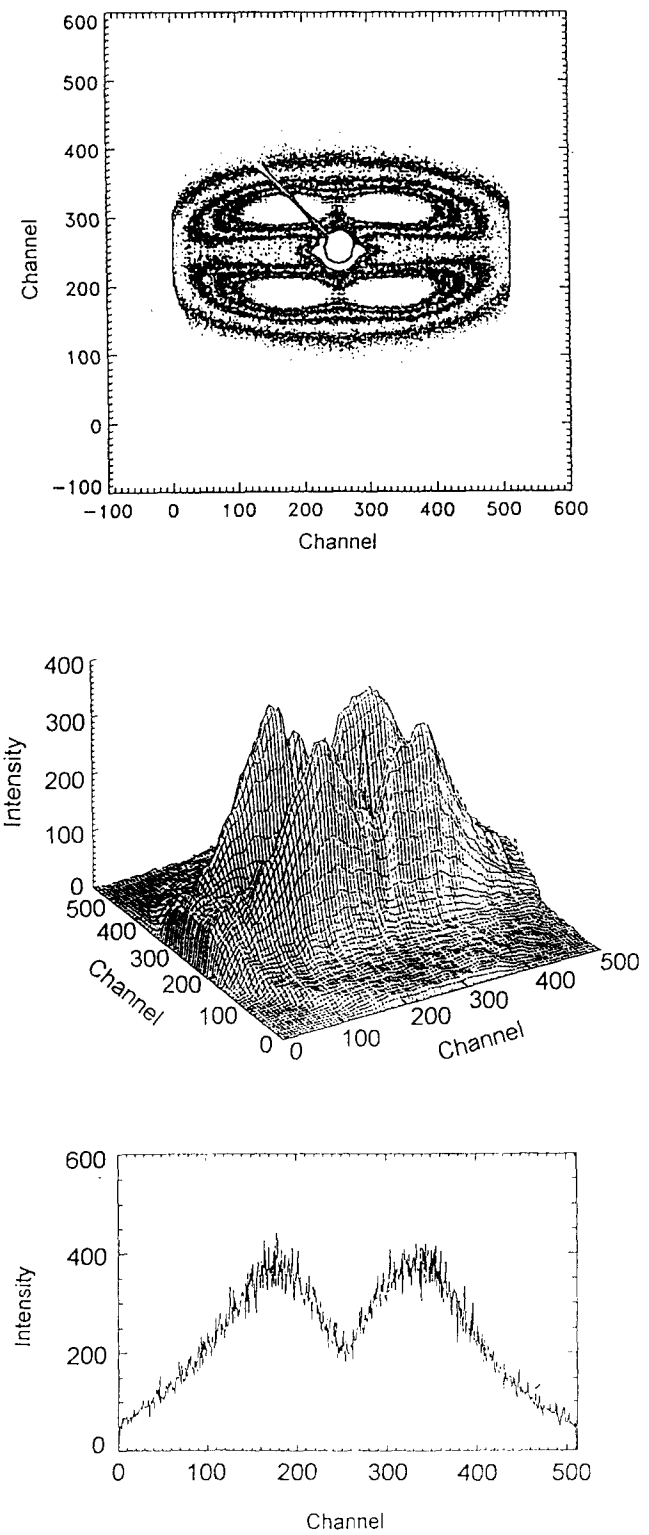

Figure 6 As for *Figure 3* but for sample 5

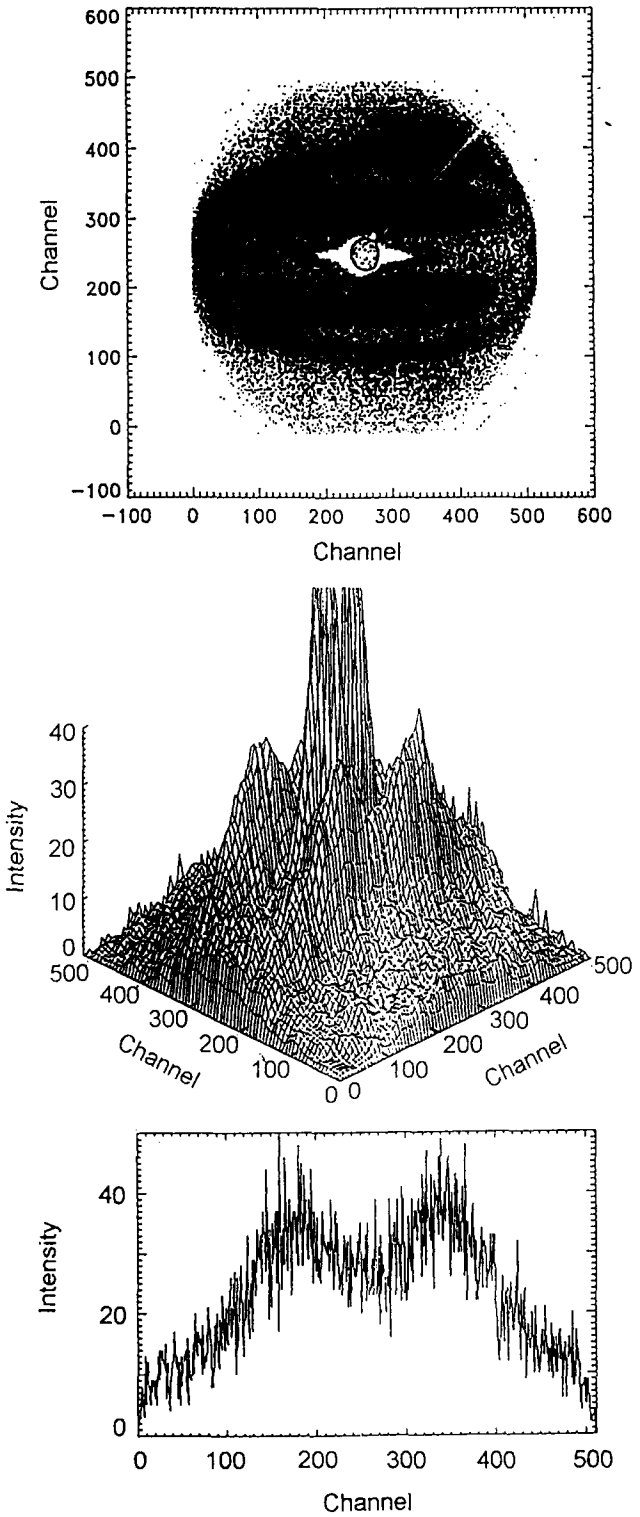

Figure 7 As for *Figure 3* but for sample 9

Table 3 Long periods determined from Kratky camera measurements with the slit perpendicular to the drawing direction

Sample	Long period L (nm)
2	15.0[a]
3	14.4
4	15.2
5	14.8
9	13.3

[a] Meridional scattering intensities are influenced by strong equatorial scattering intensities

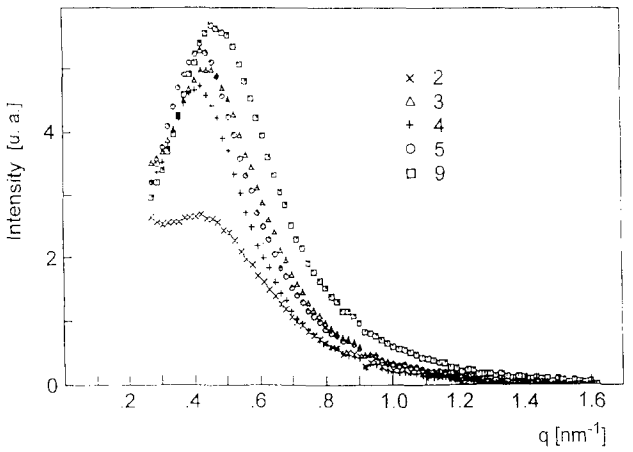

Figure 8 Slit-smeared SAXS intensity $\tilde{I}_{\perp}(b_3)$ curves of oriented semicrystalline PET samples 2, 3, 4, 5 and 9 with the incident beam perpendicular to the film plane

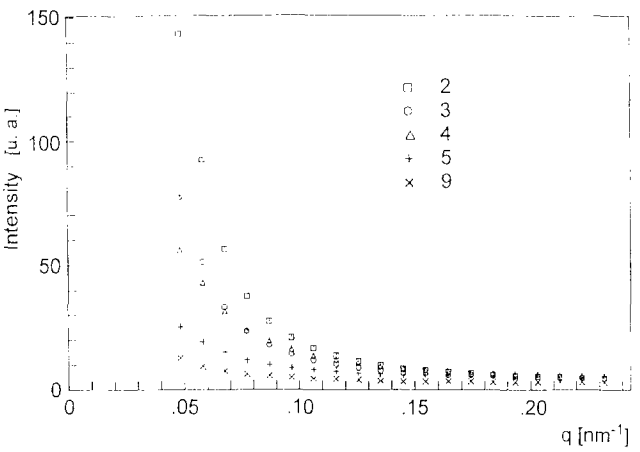

Figure 9 Slit-smeared SAXS intensity $\tilde{I}_{\parallel}(b_2)$ curves of oriented semicrystalline PET samples 2, 3, 4, 5 and 9 with the incident beam perpendicular to the film plane

DISCUSSION

Four-point SAXS patterns (two drawing steps)

The cold-drawn samples 1 and 8 are non-crystalline according to WAXS and SAXS studies. Further drawing of samples 1 and 8 yields highly oriented and semicrystalline structures, i.e. those of samples 2 and 9. In both cases four-point SAXS patterns are obtained. The meridional reflexes detected are symmetrical with respect to the layer line. These patterns come from a lamellar structure where the normal to the lamellae is inclined with respect to the drawing direction[2,12]. The corresponding inclination angle ϕ (see *Figures 10* and *11*) denotes the angle between the normal to the lamellae and the drawing direction and is given in *Table 2* for various samples. To explain the straight layer line observed, there are at least two possibilities. One argument is based on the three-dimensional paracrystalline macrolattice discussed by, for example, Fronk and Wilke[13]. The second argument supposes fluctuations of both the long period and the lamellar orientation, whereby the lamellae stacks are inclined only very slightly ($\alpha \approx 0°$) (see *Figure 10*) Pakula *et al.*[12] described a straight layer line in the scattered intensity distribution using a simplified model of a one-dimensional assembly of cylindrical domains in

which the lattice vector is parallel to the drawing direction ($\alpha \approx 0°$) and the particle vector is inclined to the lattice vector ($0 \leqslant \phi \leqslant 90°$). Stockfleth *et al.*[2] also supposed $\alpha \approx 0°$ to get a straight layer line for oriented PET. In accordance with other work[2,12], for samples 2 and 9 we suppose inclined lamellae ($\phi \neq 0°$) with only a small inclination of the lamellae stacks ($\alpha \approx 0°$). The half-width (*Table 2*) of the scattering peak along the meridional layer line contains information about the length of the lamellae as well as the orientation distribution of the normal to the lamellae with respect to the drawing direction (x_3) parallel to b_3. In agreement with Pakula *et al.*[12], we conclude the existence of comparatively short lamellae for samples 2 and 9.

Both samples differ strongly concerning the drawing stress, which was applied in the second drawing step (*Table 1*). The 3.5 times larger stress in the case of sample 2 yields a larger lamellar periodicity L along the drawing direction and a slightly smaller inclination angle ϕ obtained from two-dimensional SAXS (*Table 2*). The differences in L were confirmed by one-dimensional SAXS using the collimation slit perpendicular to the drawing direction (see *Figure 8* and *Table 3*). Compared with L for isothermally crystallized PET which belongs to the same molecular weight range ($L = 9.5$–17.1 nm for $M_v = 37\,200$ according to Groeninckx *et al.*[14] and $L = 7$–11 nm for $M_w = 33\,000$ according to Cruz *et al.*[15]), the SAXS long periods L of samples 2 and 9 are large.

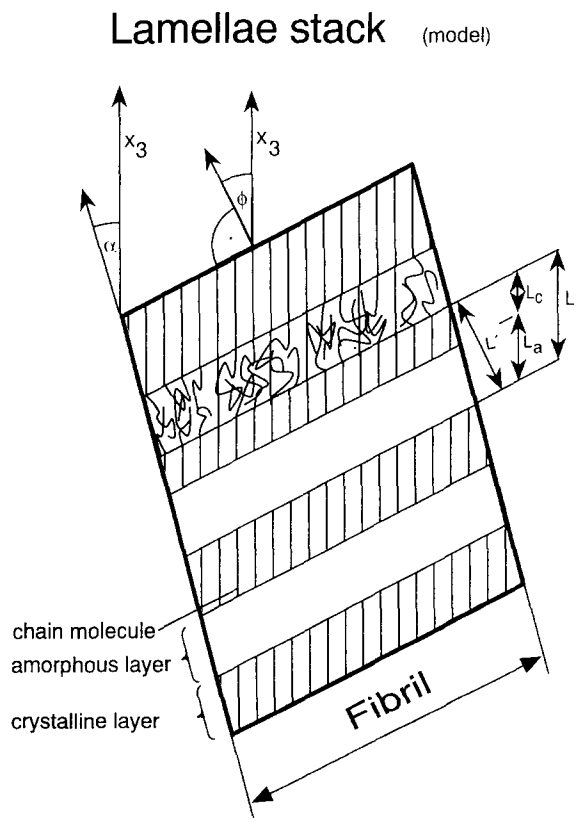

Figure 10 Model of a lamellae stack

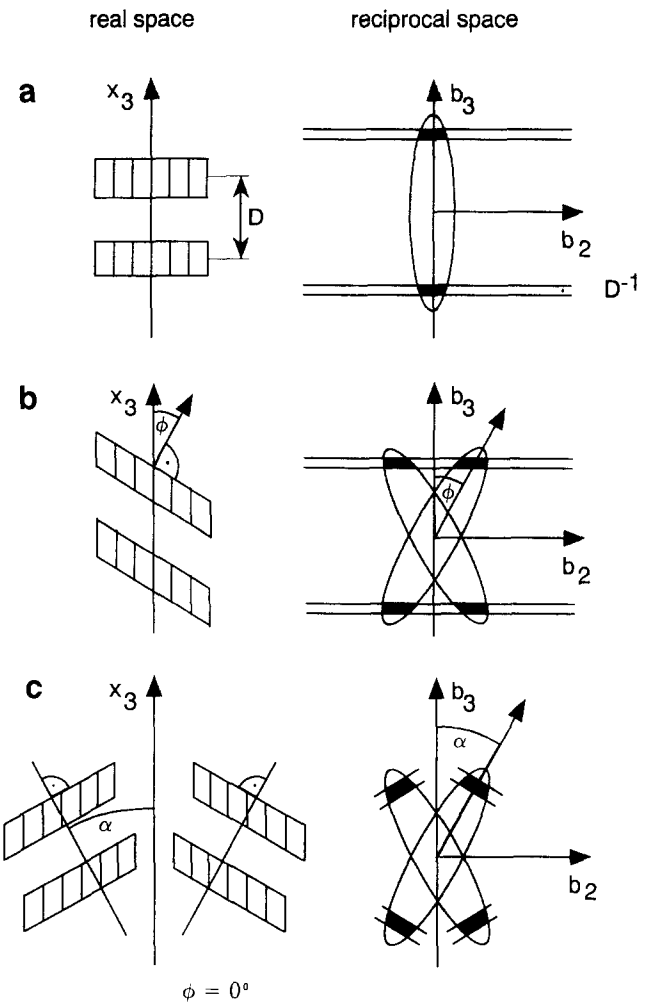

Figure 11 Supposed lamellar structures of the drawn PET samples using ϕ and α as the angles of the normal to the lamellae and the fibril axis, respectively, with respect to the drawing direction x_3. (a) An inclination angle $\phi = 0°$ yields two-point patterns for samples 3 and 4. (b) Inclination angles $\phi \neq 0°$ and $\alpha = 0°$ yield four-point patterns for samples 2 and 9. (c) Inclination angles $\phi = 0°$ and $\alpha \neq 0°$ can yield four-point patterns with inclined meridional layer line reflexes

The lamellar periodicity L' along the normal to the lamellae, which was calculated from L by way of equation (6), is somewhat larger for sample 2 than for sample 9. As a result of $\phi \neq 0°$, both samples reveal $L' < L$ (*Table 2*). In *Figure 11b* a schematic representation of the supposed lamellar structures for samples 2 and 9 is given. We assume an inclination of the normals to the lamellae with respect to the drawing direction x_3 by the angle ϕ, whereby the resulting lamellae stacks are nearly parallel to x_3. Furthermore[12], there are fluctuations in the lamellae spacing $\Delta D/D$. The interpretation of the scattering patterns (*Figure 11*) is based on a superposition of the form factor, dependent on the interparticle distances and the lattice factor, dependent on the shape, size and orientation of the individual particles, according to Pakula *et al.*[12].

As shown in *Figures 3* and *7*, samples 2 and 9 reveal strong equatorial scattering intensities. With reference to other work[3,4], these intensities are due to the occurrence of submicroscopic voids, which are phases of lower density that are located between the fibrils (lamellae stacks). From Kratky camera measurements (*Figure 9*) at small scattering vectors q, larger intensities are detected

for sample 2 than for sample 9. We assume that a decrease in the intensity is affected by a shift of the scattering curve towards lower q values, and therefore the diameter of the craze fibrils is larger than seen at a scattering vector q of 0.05 nm^{-1}. Craze formation is not within the scope of the present paper and the results will be discussed elsewhere.

Two-point SAXS patterns (three drawing steps)

We also investigated samples drawn in three steps (samples 3 and 4), which were obtained by further drawing of sample 2 at temperatures of 200 and 230°C, respectively (*Figure 1*). For both samples 3 and 4, two-point SAXS patterns were detected (*Figures 4* and *5*). With respect to *Figure 11a* we propose for these samples a lamellar structure where the normal to the lamellae is parallel to the drawing direction, i.e. $\phi = 0°$. Comparing the inclination angle $\phi = 45.4°$ for sample 2 with $\phi = 0°$ for samples 3 and 4 (*Figures 3–5*), an extraordinarily large change in ϕ is found with drawing (*Table 2*). We notice that such a large change in ϕ can occur even for highly oriented and semicrystalline structures like sample 2. These changes in ϕ are effected by increases in the drawing stress of about 35 and 50 MPa in the third drawing step for samples 3 and 4, respectively. Compared with the total drawing stress of 350–400 MPa (*Table 1*), these seem to be small stress increases. Taking into account that each drawing procedure was performed near the stress limit at each temperature, the extremely large stress in the third drawing step, accompanied by a significant increase in the draw ratio of nearly 15% (*Table 1*), was only achievable through a temperature jump. From WAXS studies on these samples[6] it is known that the crystallites are nearly perfectly aligned with respect to the drawing direction. Therefore, the drawing during the third step effects a turn of the normal to the lamellae into the drawing direction without any change in crystallite orientation. Stockfleth *et al.*[2] described for PET a transition from four-point into two-point patterns during deformation as a consequence of different deformation modes. They explained that for inclined lamellae stacks and temperatures above the glass transition, lamellar slips play an essential role. It has to be mentioned that sample 3 did not always show $\phi = 0°$, and in some cases $\phi \neq 0°$ was also found. Therefore, the structural changes effected in the third drawing step of sample 3 are not so uniform as those in sample 4, which was drawn under somewhat stronger conditions (*Table 1*).

Moreover, comparison of samples 2, 3 and 4 demonstrates that further drawing has minimized the equatorial scattering intensities (*Figure 9*). We suppose that this minimization is due to an increase in the diameter of the craze fibrils, which would shift the scattering curve towards smaller values of the scattering vector q.

Four-point SAXS patterns with bent reflexes (two drawing steps)

Sample 5 was drawn in two steps and reveals a four-point SAXS pattern (*Figure 6*). In contrast to samples 2 and 9, the meridional layer line reflexes of sample 5 are bent in a slightly convex fashion. Such a scattering pattern is usually found for structures with inclined lamellae stacks[12,13]. According to Pakula *et al.*[12], the proposed structure of sample 5 reveals features of inclined lamellae and inclined lamellae stacks (*Figures 11b* and *11c*).

Concerning the final drawing conditions (400 MPa, 200°C), sample 5 is comparable with samples 3 and 4 (see *Figure 1*). The total draw ratio achieved for each of these samples is close to 7.3, but their superstructures are quite different. The normal to the lamellae for sample 5 is inclined with respect to the drawing direction by 52°, in contrast to $\phi = 0°$ for samples 3 and 4. These structural differences can be explained in terms of the large differences in the drawing procedure. Concerning sample 5, the total drawing stress of 400 MPa was applied suddenly in the second drawing step, starting from 15 MPa after the first step (*Figure 1*). This means that the complete transition from a non-crystalline into a semicrystalline structure ($L_{\bar{1}05}/L \approx 30\%$), including a further improvement of the chain orientation, was achieved in only one step. In contrast to sample 5, samples 3 and 4 were drawn several times during the second (160°C) as well as the third (200 or 230°C) step under a stepwise increase in the drawing stress ($\sigma \approx 50$ MPa), as shown in *Table 1*. Among all the semicrystalline PET structures investigated, sample 5 reveals the largest inclination angle.

CONCLUSIONS

Two-dimensional small-angle X-ray scattering studies on uniaxially drawn PET films possessing a nearly perfect crystallite orientation with regard to the drawing direction reveal a lamellar structure with stacks of comparatively short crystalline lamellae. The lamellar structure even of highly oriented and semicrystalline PET can be changed by further drawing steps. By varying the temperature, stress and the number of steps in the multistep zone-drawing procedure, a draw ratio in the range 5.4–7.3, a lamellar periodicity along the drawing direction of 14.2–16.6 nm and an angle between the normal to the lamellae and the drawing direction of 0–52° are obtained. Starting from a non-crystalline structure with a high chain orientation along the drawing direction, a transition from a semicrystalline structure with inclined lamellae ($\phi = 45.4°$) into a lamellar structure with $\phi = 0°$ is revealed. Despite this tilting of the lamellae, the c axis of the crystallites remains nearly parallel to the drawing direction.

The use of a two-dimensional detector in conjunction with point collimation is particularly advantageous for the investigation of oriented structures, especially in the case of inclined lamellae where the scattering intensities are located apart from the meridian.

ACKNOWLEDGEMENTS

The author would like to thank Dr T. Pakula and Dr V. Abetz for helpful discussions. The kind cooperation and technical assistance of M. Bach, T. Wagner and Ch. Crook are also gratefully acknowledged.

REFERENCES

1 Fischer, E. W., Goddar, H. and Schmidt, G. F. *Makromol. Chem.* 1968, **118**, 144
2 Stockfleth, J., Salamon, L. and Hinrichsen, G. *Colloid Polym. Sci.* 1993, **271**, 423
3 Bonart, R. *Kolloid Z. Z. Polym.* 1966, **211**, 14

4 Paredes, E. and Fischer, E. W. *Makromol. Chem.* 1979, **180**, 2702
5 Göschel, U. *Acta Polym.* 1989, **40**, 23
6 Hofmann, D., Göschel, U., Walenta, E., Geiß, D. and Philipp, B. *Polymer* 1989, **30**, 242
7 Göschel, U. *Polymer* 1992, **33**, 1981
8 Fischer, E. W. and Fakirov, S. *J. Mater. Sci.* 1976, **11**, 1041
9 Biangardi, H. J. and Zachmann, H. G. *J. Polym. Sci., Polym. Symp.* 1977, **58**, 169
0 Nobbs, J. H., Bower, D. I. and Ward, I. M. *Polymer* 1976, **17**, 25
11 Peszkin, P. N. and Schultz, J. M. *J. Polym. Sci., Polym. Phys. Edn* 1986, **24**, 2591
12 Pakula, T., Saijo, K., Kawai, H. and Hashimoto, T. *Macromolecules* 1985, **18**, 1294
13 Fronk, W. and Wilke, W. *Colloid Polym. Sci.* 1985, **263**, 97
14 Groeninckx, G., Reynaers, H., Berghmans, H. and Smets, G. *J. Polym. Sci., Polym. Phys. Edn* 1980, **18**, 1311
15 Cruz, C. S., Stribeck, N., Zachmann, H. G. and Balta' Calleja, F. J. *Macromolecules* 1991, **24**, 5980